

Interaction between vortices and ferromagnetic microstructures in twinned cuprate/manganite bilayers

F. Laviano,* L. Gozzelino, R. Gerbaldo, G. Ghigo, and E. Mezzetti

*Department of Physics, Politecnico di Torino, Corso Duca degli Abruzzi 24, 10128 Torino, Italy
and INFN Sezione di Torino, Via P. Giuria 1, 10125 Torino, Italy*

P. Przyslupski, A. Tsarou, and A. Wisniewski

*Institute of Physics, Polish Academy of Sciences, Aleja Lotnikow 32/46, Warsaw 02-668, Poland
(Received 13 October 2006; revised manuscript received 12 June 2007; published 4 December 2007)*

The role of magnetic microstructures and correlated defects on magnetic field and supercurrent distributions in cuprate/manganite bilayers was studied using the magneto-optical imaging technique. For this purpose, bilayer structures were deposited on twinned LaAlO_3 substrates. Experimental results indicate that different magnetic patterns could be induced in the ferromagnetic $\text{La}_{1-x}\text{Sr}_x\text{MnO}_3$ film deposited on twinned substrate. Depending on the induced magnetic microstructure of the ferromagnetic layer, the vortex pinning due to the twin-boundary network in the $\text{YBa}_2\text{Cu}_3\text{O}_{7-\delta}$ layer becomes strongly modulated. In particular, the force acting on vortices due to the interaction with macroscopic magnetic domains, having out-of-plane tilted magnetization, was locally measured. The measurements at low temperature show that the magnetic interaction slightly contributes to the total pinning force density over the domains. It turns out that the alternating out-of-plane magnetization induces spontaneous counterflowing supercurrent loops in the superconducting layer. Finally, reference measurements made on a bilayer with nonferromagnetic manganite ($\text{Nd}_{0.5}\text{Sr}_{0.5}\text{MnO}_3$) show that twin boundaries without localized magnetic moments produce homogeneous and strong vortex pinning in the twinned bilayers.

DOI: [10.1103/PhysRevB.76.214501](https://doi.org/10.1103/PhysRevB.76.214501)

PACS number(s): 74.78.Fk, 74.25.Qt, 75.47.Lx, 75.70.Cn

INTRODUCTION

Superconducting/ferromagnetic (SC/FM) heterostructures have attracted much attention for experimental and theoretical studies due to the novel physical phenomena caused by the interplay between two competing order parameters.¹ Much interest is devoted to study the magnetic interaction between the layers. Bulaevskii *et al.*² suggested that the presence of out-of-plane magnetic moments, with alternating magnetic domains in the FM layer, could enhance the pinning of the superconducting vortices in the SC layer. Experimental results show an increased pinning in SC/FM bilayers,³⁻⁵ although details of the magnetic domain structure of the FM layer were not investigated. Therefore, it is reasonable to expect that various domain topologies and correlated defects⁶ cause complex electromagnetic interactions between the magnetic microstructure and vortices.

High-resolution magneto-optical (MO) technique was successfully used to probe the phase transition of the magnetic pattern in a $\text{La}_{0.67}\text{Ca}_{0.33}\text{MnO}_3$ thin film deposited on SrTiO_3 substrate.⁷ The measurements have shown that a substrate martensitic transition induces localized out-of-plane magnetic moments in the manganite layer. Our previous studies by means of the MO imaging technique on $\text{YBa}_2\text{Cu}_3\text{O}_{7-\delta}/\text{La}_{1-x}\text{Sr}_x\text{MnO}_3$ (YBCO/LSMO)⁸ bilayers grown on twinned LaAlO_3 substrate (LAO) indicate the appearance of spontaneous vortices and antivortices in the SC layer, induced by out-of-plane magnetic moments which are localized at twin boundaries (TB's) in the FM layer. This experiment was performed for two doping levels of the LSMO system ($x=0.33$ and 0.115).⁹

In this paper, we further investigate the local interaction between different magnetic microstructures and vortices in

epitaxial YBCO/ $\text{RE}_{1-x}\text{Sr}_x\text{MnO}_3$ bilayers, grown on twinned LAO substrates. The magnetic field distribution of each layer was visualized by high-resolution MO imaging in order to understand how the vortex-pinning potential of TB's is modified by the localized magnetic moments and what is the influence of the magnetic domains on vortex pinning (far from TB's). Therefore, the local measurement of the critical current for vortices diffusing over single magnetic domains in YBCO/LSMO bilayers gives us the local contribution of the magnetic interaction between vortices and monodomains with out-of-plane tilted magnetization. Moreover, we observed that the alternating magnetic pattern in the LSMO layer spontaneously induces macroscopic counterflowing supercurrent loops in the YBCO film.

Finally, for a direct comparison of the vortex pinning in twinned heterostructures with and without the FM ground state, we present the MO imaging of YBCO/ $\text{Nd}_{1-x}\text{Sr}_x\text{MnO}_3$ (NSMO) bilayer, because the ground state of NSMO, with $x=0.5$ doping level, is antiferromagnetic with Néel temperature of about 140 K (due to real space ordering of Mn^{3+} and Mn^{4+} ions in different sublattices).¹⁰ This sample is also deposited on twinned LAO substrate in order to demonstrate that without ferromagnetism in the manganite layer, the TB's are not able to generate any spontaneous flux structure, but only produce homogeneous strong pinning of vortices in the SC layer.

EXPERIMENTAL DETAILS

All the bilayers were grown *in situ* on LAO single-crystal substrates by multitarget high-pressure dc sputtering from the stoichiometric targets.¹¹ The LAO substrate naturally dis-

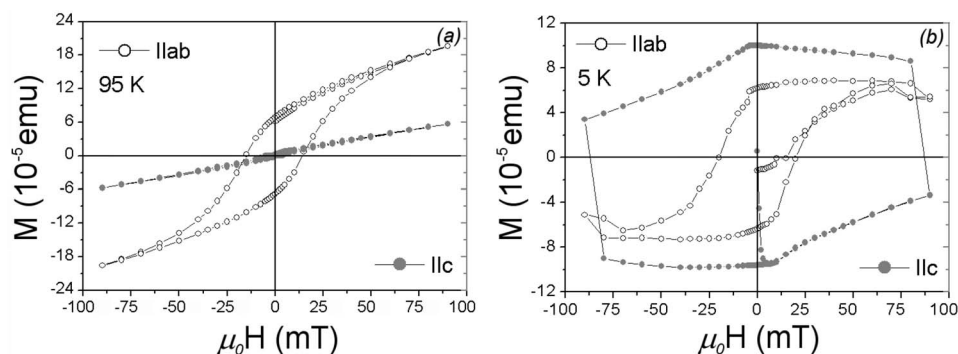


FIG. 1. Bulk magnetization of the bilayer measured in a superconducting quantum interference device magnetometer. (a) Above the YBCO T_c , the magnetic signal is coming only from the LSMO layer and it is clearly demonstrated that the easy axis is in-plane aligned. (b) A net out-of-plane magnetization component develops, at low temperature, due to the vortices nucleated in the SC layer.

plays a large number of coherent TB's,¹² organized either in parallel families or in a zigzag structure. Most of the TB's in the substrate propagate up to the top layer of the heterostructure.

We studied YBCO/NSMO bilayers (the SC top layer is 50 nm thick, whereas the manganite layer is 100 nm thick), with the NSMO system at $x=0.5$ doping level¹³ and YBCO/LSMO bilayers with $x=0.115$ ($T_{Curie} \sim 180$ K, 100 nm thick FM layer, 50 nm thick SC top layer, with critical temperature T_c around 89 K). X-ray data¹⁴ show that the LSMO layer is relaxed and the measurement of the bulk magnetization¹⁵ demonstrates that the FM layer has the easy axis of magnetization in-plane aligned [see Fig. 1(a)], whereas a net out-of-plane component is generated only by the SC layer, as shown in Fig. 1(b).

High-resolution MO imaging of the magnetic distribution in opaque materials is obtained using the MO-active indicators.^{16,17} As indicators, we have used Bi-doped iron garnet films with in-plane magnetization,¹⁸ grown by liquid-phase epitaxy on optical substrates and covered with thin silver mirrors.¹⁹ The local magnetization of the indicator is rotated out of the plane, depending on the local magnetic field induced by the measured sample. The local magnetization rotation is directly imaged as light intensity modulation by the Faraday effect and by the light polarization analysis. In the MO measurements here presented, the bright contrast, with respect to the average gray level, corresponds to the local magnetic moment directed toward the reader and the dark contrast represents an out-of-plane component of opposite direction. To achieve the quantitative MO imaging of the magnetic field distribution and its model-independent deconvolution into the supercurrent distribution,²⁰ the sample should be in film form and its surface should be smaller than the optical frame size, due to the requirements of the nonlinear calibration procedure.²¹ For this reason, the YBCO film of the bilayer with the insulating LSMO was patterned by UV photolithography and by chemical wet etching in a HCl/H₂O(0.3%) solution. In order to evaluate the supercurrent distribution in the SC layer, the manganite layer was magnetically polarized above the SC T_c by an in-plane magnetic field and then the zero-field background pattern was subtracted from each MO frame, measured with a nonzero out-of-plane applied field. Using such a procedure, we ob-

tained the image of the local magnetic field generated only by the supercurrent density that is established in the SC layer as a consequence of the applied magnetic field, i.e., critical currents in the vortex penetrated regions and Meissner currents in the flux-free part.

RESULTS AND DISCUSSION

Different magnetic patterns occurring in the insulating LSMO layer on twinned LAO substrate are presented in Fig. 2. The YBCO layer was etched in a 200 μm diameter disk: its edge is visible on the right of Figs. 2(a) and 2(b). The pattern of Fig. 2(c) corresponds to the area of the FM layer just under the other pictures.

These patterns were induced by applying an in-plane magnetic field of 100 mT, parallel [in Fig. 2(a)] and antiparallel [in Fig. 2(b)] with respect to the direction indicated by the black arrow in Fig. 2(c). In the last pattern, a magnetic field gradient (generated with the help of permanent magnets) was applied in order to depin the domain walls (DW's) from TB's, because the local coercitivity is greatly enhanced at correlated defects.²² The magnetization of the domains is slightly tilted out of plane (much less than the saturation magnetization), in Figs. 2(a) and 2(b), and these two patterns show opposite out-of-plane magnetic moments in the same areas (schemes of magnetization are reproduced below each measurement). On the contrary, the magnetization of the domains is completely in-plane aligned in Fig. 2(c) and single DW's (charged walls)⁶ are visible in between the TB's. In any case, the LSMO layer has a net magnetization only in-plane aligned as shown in the measurement of the total magnetic moment presented in Fig. 1 and the small out-of-plane component when present has alternating sign in adjacent domains.

Since the magnetic field in the nonsuperconducting core of the vortex is of the order of the lower critical field, B_{c1} (for YBCO around 15 mT), and the intrinsic coercitivity was less than this value,²³ it would be reasonable that the vortices exert a dragging force onto single DW's. In this respect, the TB network turns out to be useful for pinning the multidomain pattern induced with an external magnetic field. Therefore, the pattern with alternating out-of-plane domains and pinned DW's, e.g., like the one shown in Fig. 2(b), is appro-

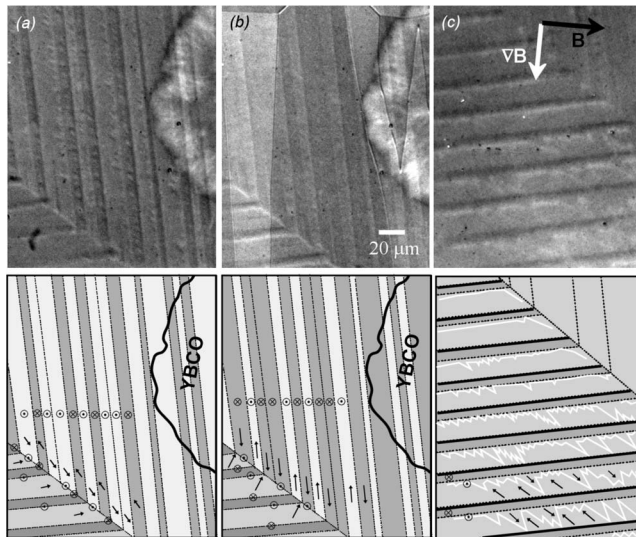


FIG. 2. Magnetic field distributions of a YBCO/LSMO bilayer in different magnetization states, induced by applying in-plane magnetic fields of opposite directions and a magnetic field gradient in order to depin single DW's. Directions of the applied field and field gradient are shown in (c). Below each measurement, a scheme of the magnetization vectors is presented. (a) This magnetization state displays domains with out-of-plane tilted magnetization ($T = 3.9$ K). (b) Magnetic field distribution of the same region shown in (a) but in a complementary magnetization state, i.e., the local out-of-plane component of the magnetization is tilted in the opposite direction with respect to (a). The triangular big domains on the left and on the right are due to the indicator film and must be disregarded. (c) Single DW's are induced in between TB's by the application of a strong in-plane field gradient (larger than 1 T/m).

appropriate for studying the intrinsic magnetic interaction between vortices and magnetic domains, far from strong pinning sites.

When the bilayer is cooled below T_c in nominal zero-field [zero-field cooling (ZFC)], the out-of-plane magnetic moments [distributed in the LSMO layer as depicted in Fig. 2(b)] are trapped inside the YBCO film and the spontaneously induced vortex distribution is quite uniform over the single domain area.⁹

When a uniform external magnetic field is applied perpendicular to the sample, new vortices start to nucleate at the SC edges. With increasing external field, vortices diffuse toward the central area of the sample. In the critical state profile [magnetic field map in the inset of Fig. 3(a)], modulations of the magnetic flux density are visible,⁹ because vortices generated by the applied external field repulse the spontaneous vortices of the same polarity while attract and annihilate the spontaneous antivortices in adjacent domains with antiparallel magnetization.

Apart from the modulations induced by the roughness of the sample edge, the vortex density gradient crossing adjacent alternating domains does correspond to smooth changes of the local critical current. Indeed, the quantitative evaluation of the supercurrent density distribution [shown in Fig. 3(a)] demonstrates slight modulations of the pinning force density in the critical state.

In order to make the quantitative estimation of the local pinning variation, we traced linear profiles of magnetic field

and supercurrent, Figs. 3(b) and 3(c), along the dotted segments indicated in Fig. 3(a). Minor modulations with high spatial frequency of the supercurrent in the domain bulk are due to pinning potential variations caused by isolated inclusions (as identified by the peaks of the magnetic field profile). TB's are marked by vertical dotted lines. It is remarkable that vortex pinning at TB's is not systematically maximum, presumably because the magnetization gradient at TB's (in the FM layer) induces vortex sliding.

The difference in the critical current in the bulk of adjacent domains [whose magnetization direction with respect to the applied field is labeled, in the profiles of Figs. 3(b) and 3(c), as POS for domains with an out-of-plane component parallel to the applied field and as NEG for the opposite direction of the out-of-plane component only], is of the order of 10% of the average critical current value (around 2.5×10^{11} A m⁻²), with a slight increase of the supercurrent statistically corresponding to the domains whose magnetization is antiparallel with respect to the applied field [see the histogram in Fig. 3(d)].²⁴

Taking into account that the intervortex interaction should be negligible for the value of the uniform applied field (corresponding to an induction field of 4.5 mT),²⁵ it results that the monodomain with an out-of-plane tilted magnetization (corresponding to a local induction of the order of 1 mT perpendicular to the film plane) contributes to the vortex-pinning force density less than 10% with respect to the pinning exerted by crystal defects (such as dislocations), in the YBCO layer.

It is worthy to note that the current theory of the magnetic pinning² takes into account a magnetic pattern with an average domain size smaller than the intervortex distance; therefore, the strong pinning results from the matching of the characteristic lengths between the flux line lattice and the domain structure.

We also observed that in the central part of the sample, inside the area not reached by the vortices generated by the external applied field, the screening current loop is split into different domains. These current loops directly reflect the alternating out-of-plane domain pattern: adjacent domains with opposite magnetization trigger counterflowing loops [see the line profile in Fig. 3(e)]. Such supercurrent loop pattern is similar to the topological instability model predicted by Erdin *et al.*,²⁶ according to which the splitting of supercurrent loops and of magnetic domains should naturally occur for both layers, but here the alternating magnetic pattern is present above the YBCO T_c and therefore it induces an inhomogeneous local field during cooling that forces counterflowing screening loops in the SC layer.

In order to verify that the observed magnetic field and supercurrent modulations at TB's are only due to the out-of-plane tilted magnetic moments in the FM layer, we present the MO imaging of a bilayer with nonferromagnetic manganite. The TB network due to the LAO substrate is visible in Fig. 4(a). The magnetic field distribution after nominal ZFC of a 5×10 mm² YBCO/NSMO bilayer is presented in Fig. 4(b). In this bilayer, no FM component was detected below 100 K and the system presumably goes to an antiferromagnetic ground state at low temperatures.¹⁰ The slight dark contrast in the magnetic field map in Fig. 4(b) demonstrates that

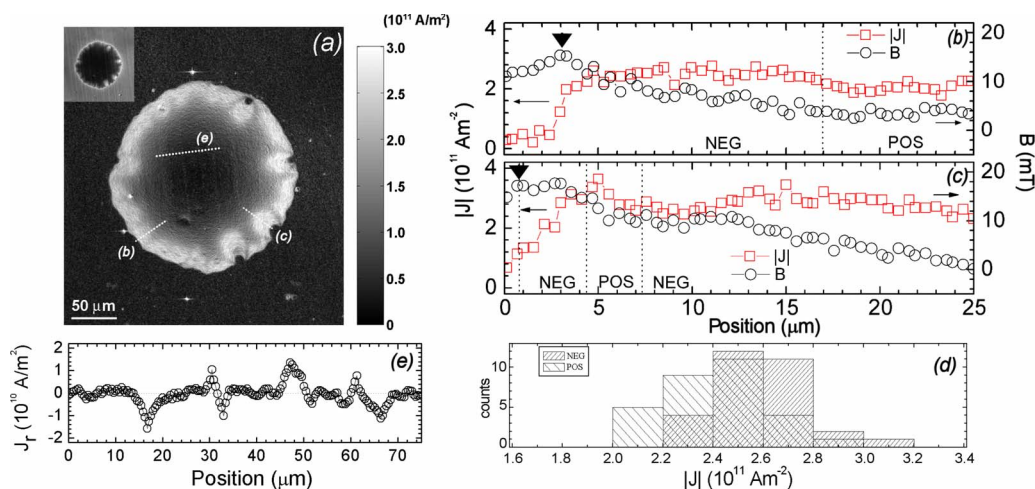


FIG. 3. (Color online) (a) Supercurrent density modulus distribution at $T=4.2$ K and $\mu_0 H_{\text{app}}=4.5$ mT, after ZFC. The disk shaped YBCO film shows edge roughness. In the inset, the corresponding distribution of the magnetic field is presented. (b), (c), and (e) are supercurrent density (squares) and magnetic field (circles) line profiles traced along the corresponding dotted segments in the supercurrent density map in (a). Dotted vertical lines in (b) and (c) mark the TB position and the downward triangle indicates the sample edge. The labels POS and NEG indicate that the out-of-plane magnetization component of the domain is directed parallel or antiparallel to the applied field, respectively. (d) Distributions of the current density values corresponding to POS and NEG domains (60 areas). The mean current density over the POS domains is 2.403×10^{11} A m $^{-2}$, whereas over NEG domains, it is 2.577×10^{11} A m $^{-2}$. For (e), data points are taken from the radial component (magnitude and sign) of the supercurrent distribution, along the corresponding dotted line traced in (a).

a coherent Meissner state establishes in order to screen the small residual field applied after the magnetic shield was removed and the electromagnet was inserted over the cryostat (its residual field is less than 0.2 mT). No localized magnetic flux, trapped in the YBCO film, was observed. When a uniform external field is applied (perpendicular to the bilayer), vortices start to enter the sample from the edges and they become pinned by the crystal defects, forming a critical gradient, as presented in Fig. 4(c). This critical state profile is modulated by the sample edge roughness and by the discontinuities in the pinning potential distribution (e.g., scratches). As expected, the TB network in the YBCO/NSMO bilayer displays strong and homogeneous pinning²⁷ over the whole sample.

CONCLUSIONS

We have studied the interaction of superconducting vortices with magnetic domains and DW's in twinned SC/FM perovskite bilayers. By means of magnetic field imaging, we demonstrated that TB's tailor the magnetization state of the manganite and that the interaction between TB's and vortices is locally modulated, depending on the induced magnetic microstructure in the FM layer. These magnetic patterns are always frozen in the SC layer when cooling below the SC T_c .

Measurements were focused on the magnetic pattern with alternating out-of-plane domains (several microns wide), separated by TB's. In this case, either enhancement or depression of the local supercurrent was observed in the critical state part and these modulations are of the order of 10% of the average critical current. Furthermore, a strong modulation of the supercurrent is spontaneously established in the central part of the sample due to the occurrence of macroscopic counterflowing screening current loops.

Moreover, experimental results obtained on a bilayer with nonferromagnetic NSMO manganite demonstrate that, on the contrary, the TB's alone are not able to induce any spontaneous flux structure in the SC layer and they produce homogeneous pinning in the heterostructure without localized ferromagnetic moments.

It results that the strong and inhomogeneous enhancement of the DW coercivity due to correlated defects is a dominant parameter for the equilibrium magnetic pattern of these hybrid heterostructures. The localized out-of-plane magnetic moments in the FM layer cause spontaneous flux nucleation and pinning modulations in the SC layer; therefore, the interaction of the magnetic microstructure with correlated defects in magnetic perovskite compounds deserves special at-

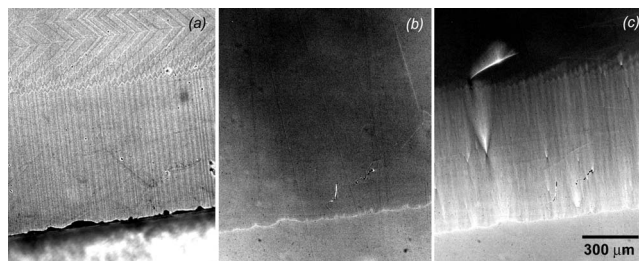


FIG. 4. (a) Optical picture of the YBCO/NSMO bilayer surface obtained with linearly polarized light. Both parallel and zigzag families of coherent TB's are clearly visible. (b) MO imaging of the magnetic field distribution in the YBCO/NSMO bilayer [same region as shown in (a)], after ZFC, at $T=4.2$ K. The dark contrast area represents the region screened by the Meissner currents due to the environment field. (c) MO image of the magnetic field distribution in YBCO/NSMO bilayer, after ZFC, and the application of a set of increasing out-of-plane magnetic fields ($T=4.2$ K, $\mu_0 H_{\text{app}}=4.6$ mT).

tention both for fundamental and for applicative studies.

ACKNOWLEDGMENTS

This work was partially supported by the Programme of Scientific and Technological Cooperation between the Italian

Republic and the Republic of Poland 2004–2006. This work was also supported by the Polish Ministry of Science and Higher Education under a project for the years 2006–2009 (MNiSW-1 P03B 122 30). The Italian partners acknowledge the contribution of the MIUR-PRIN Project No. 2004037901.

*High resolution data are available upon request from the corresponding author: francesco.laviano@polito.it

¹A. I. Buzdin, *Rev. Mod. Phys.* **77**, 935 (2005).

²L. N. Bulaevskii, E. M. Chudnovski, and M. P. Maley, *Appl. Phys. Lett.* **76**, 2594 (2000).

³A. Garcia-Santiago, F. Sanchez, M. Varela, and J. Tejada, *Appl. Phys. Lett.* **77**, 2900 (2000).

⁴H.-U. Habermeier, J. Albrecht, and S. Soltan, *Supercond. Sci. Technol.* **17**, S140 (2004).

⁵J. Albrecht, S. Soltan, and H.-U. Habermeier, *Phys. Rev. B* **72**, 092502 (2005).

⁶A. Hubert and R. Schafer, *Magnetic Domains: The Analysis of Magnetic Microstructure* (Springer-Verlag, Berlin, 1998).

⁷V. K. Vlasko-Vlasov, Y. K. Lin, D. J. Miller, U. Welp, G. W. Crabtree, and V. I. Nikitenko, *Phys. Rev. Lett.* **84**, 2239 (2000).

⁸F. Laviano, L. Gozzelino, E. Mezzetti, P. Przyslupski, A. Tsarou, and A. Wisniewski, *Appl. Phys. Lett.* **86**, 152501 (2005).

⁹L. Gozzelino, F. Laviano, P. Przyslupski, A. Tsarou, A. Wisniewski, D. Botta, R. Gerbaldo, and G. Ghigo, *Supercond. Sci. Technol.* **19**, S50 (2006).

¹⁰Y. Tokura, *Rep. Prog. Phys.* **69**, 797 (2006).

¹¹P. Przyslupski, A. Wisniewski, R. Szymczak, and J. Igalson, *Czech. J. Phys.* **46**, 1355 (1996); P. Przyslupski, S. Kolesnik, E. Dynowska, T. Skoskiewicz, and M. Sawicki, *IEEE Trans. Appl. Supercond.* **7**, 2192 (1997).

¹²Eric B. McDaniel and J. W. P. Hsu, *J. Appl. Phys.* **80**, 1085 (1996).

¹³A. Tsarou, W. Paszkowicz, P. Dluzewski, M. Sawicki, and P. Przyslupski, *Acta Phys. Pol. A* **111**, 179 (2007).

¹⁴A. Chiodoni, L. Gozzelino, F. Laviano, P. Przyslupski, A. Tsarev, and A. Wisniewski, *Phys. Status Solidi C* **2**, 1644 (2005).

¹⁵P. Przyslupski, I. Komissarov, W. Paszkowicz, P. Dluzewski, R. Minikayev, and M. Sawicki, *Phys. Rev. B* **69**, 134428 (2004).

¹⁶Ch. Jooss, J. Albrecht, H. Kuhn, S. Leonhardt, and H. Kronmuller, *Rep. Prog. Phys.* **65**, 651 (2002).

¹⁷S. Dreyer, J. Norpoth, C. Jooss, S. Sievers, U. Siegner, V. Neu, and T. H. Johansen, *J. Appl. Phys.* **101**, 083905 (2007).

¹⁸L. A. Dorosinskii, M. V. Indenbom, V. I. Nikitenko, Yu. A. Ossip'yan, A. A. Polyanskii, and V. K. Vlasko-Vlasov, *Physica C* **203**, 149 (1992).

¹⁹L. E. Helseth, A. G. Solov'yev, R. W. Hansen, E. I. Il'yashenko, M. Baziljevich, and T. H. Johansen, *Phys. Rev. B* **66**, 064405 (2002).

²⁰F. Laviano, D. Botta, A. Chiodoni, R. Gerbaldo, G. Ghigo, L. Gozzelino, S. Zannella, and E. Mezzetti, *Supercond. Sci. Technol.* **16**, 71 (2003).

²¹Ch. Jooss, A. Forkl, R. Wartmann, H.-U. Habermeier, B. Leibold, and H. Kronmuller, *Physica C* **266**, 235 (1996).

²²A. J. Kurtzig, *IEEE Trans. Magn.* **6**, 497 (1970).

²³We measured an intrinsic coercivity of 10.3 kA/m. A detailed study of the domain-wall dynamics in insulating manganite films deposited on twinned substrates will be presented elsewhere.

²⁴We performed the Student's test on POS and NEG distributions taken from 60 areas in the critical state regions of the YBCO layer. The difference between the two mean values is significant with a confidence interval of 99.9%.

²⁵E. H. Brandt, *Rep. Prog. Phys.* **58**, 1465 (1995).

²⁶S. Erdin, I. F. Lyuksyutov, V. L. Pokrovsky, and V. M. Vinokur, *Phys. Rev. Lett.* **88**, 017001 (2001).

²⁷V. K. Vlasko-Vlasov, L. A. Dorosinskii, A. A. Polyanskii, V. I. Nikitenko, U. Welp, B. W. Veal, and G. W. Crabtree, *Phys. Rev. Lett.* **72**, 3246 (1994); C. A. Duran, P. L. Gammel, D. J. Bishop, J. P. Rice, and D. M. Ginsberg, *ibid.* **74**, 3712 (1995); U. Welp, T. Gardiner, D. O. Gunter, B. W. Veal, G. W. Crabtree, V. K. Vlasko-Vlasov, and V. I. Nikitenko, *ibid.* **74**, 3713 (1995).